Desalination and Water Treatment
www.deswater.com

doi: 10.1080/19443994.2013.797643

52 (2014) 3104–3114
April

Taylor & Francis
Taylor & Francis Group

Magnetic adsorbent used in combination with ultrafiltration membrane for the removal of surfactants from water

Muhammad Zahoor

Department of Chemistry, University of Malakand, Chakdara, Dir (lower), Khyber Pakhthunkhwa, Pakistan
Email: mohammadzahoorus@yahoo.com
Faculty of Chemical Engineering, Istanbul University, Istanbul, Turkey

Received 16 May 2012; Accepted 11 April 2013

ABSTRACT

Powdered activated carbon (PAC)/iron oxide composite (MAC13) was prepared and was characterized by surface area analyzer, powdered X-ray diffraction, and sigma bulk magnetization. The adsorptive parameters of the prepared adsorbent and PAC were determined for Triton X-100, N-dodecylpyridinium chloride, and sodium dodecylbenzene sulfonate. The equilibrium adsorption data matched well to Langmuir model in various concentration ranges. The effects on contact time of adsorbates on adsorbents were determined. Both adsorbents were used in hybrid manner in pilot plant with ultrafiltration membrane (UF) system. The UF membrane parameters were determined for both PAC/UF and MAC13/UF process. Although the percent retention for PAC/UF was high, was associated with some secondary problems like cake formation over membrane and blacking of pipes. These secondary problems were not observed for MAC13, as MAC13 was removed from the slurry after use through magnet. Improved permeate fluxes were observed for MAC13 as the decline in permeate flux caused by cake formation was not encountered for magnetic adsorbent. The back wash time for PAC and MAC13 was compared and was found high for PAC.

Keywords: Adsorption; Permeate flux; Percent retention; Ultrafiltration membrane

1. Introduction

The use of surfactants have increased tremendously from few decades. In the year 2000, its world wide production was 17 million tons. Due to their world wide use and strong resistance to biological degradation, their concentration in water bodies has drastically increased [1]. Surfactants are used in several domains such as textiles, fibers, food, paints, polymers, cosmetics, pharmaceuticals, microelectronic, mining, oil recovery, and pulp-paper industries to name just few. Surfactants are harmful to human beings, fishes, and aquatic flora. They can cause pathological, physiological, and biochemical effect on aquatic animals. In aquatic plants, they cause break-up of the chlorophyll–protein complex, damage the cell and other organelles membrane, and delay in metabolism and growth [2]. They are also responsible to cause foams in rivers and effluent treatment plants and to reduce the quality of water [3]. Due to their hazardous effects, surfactants should be removed

from industrial effluents and other wastewater emission systems. The removal of these materials from industrial wastewaters is one of the major environmental problems because of the difficulty of treating such water by conventional treatment methods.

The various methods employed for the removal operations of surfactants from water are; chemical and electrochemical oxidation [4,5], chemical precipitation [6,7], photo catalytic degradation [8–10], adsorption [11–13], biological methods [14–16], and membrane technology [17–19]. Amongst these employed methods, adsorption is the most successful method for the removal of surfactants from water. However, adsorption processes are not rapid and one has to wait long for the settling of adsorbent. Membrane processes have been in use for a few decades and have proved to be efficient in drinking water production. However, fouling by organic contaminants and concentration polarization affects the efficiencies of these processes. To minimize fouling pretreatment like coagulation followed by sedimentation [20–22], coagulation followed by dissolved air flotation [23], and activated carbon adsorption [24,25] were performed. The pretreatment with powdered activated carbon (PAC) is considered the most effective method for foul control [26–29]. However, it is associated with some secondary problems like formation of cake over membrane, and blackening of the pipes and other accessories of the hybrid systems. The cake formation over membrane causes a decline in permeate flux which in turn leads to loss of water and electricity in back washing of the membrane and replacement of the blackened pipes and other accessories of the hybrid system in premature period [30–33].

Keeping in view the problems associated with adsorption–membrane hybrid processes, magnetic activated carbon, which was an impregnated composite of PAC and iron oxide in 1:2 ratio, was prepared by the method devised by Olivera [34] and was used for fouling control in the hybrid processes in our previous work. However, due to low surface area of magnetic activated carbon (1:2), the permeate fluxes were comparable to that PAC [33].

To get high surface area of PAC/iron oxide composite and consequently high permeate flux than that for PAC in hybrid processes, magnetic activated carbon in 1:3 ratio (MAC13) was prepared and was used in combination with ultrafiltration (UF) membrane for foul control. MAC13 and PAC were compared for foul control and removal efficiencies of surfactants, Triton X-100, N-dodecylpyridinium chloride, and sodium dodecylbenzene sulfonate (SDBS).

2. Materials and methods

Triton X-100 was obtained from Merck while SDBS and N-dodecylpyridinium chloride were obtained from Sigma Aldrich. All the chemicals were of analytical grade. UF membranes (polyethersulfone) were purchased from IMT, The Netherland. The characteristic properties of the UF membrane are given in Table 1. The PAC (surface area $1150\,m^2\,g^{-1}$) was obtained from Norit. The physical parameters of PAC are given in Table 2. The adsorbent MAC13 was prepared by mixing 200 mL of $FeCl_3$ (28 m mol) and $FeSO_4$ (14 m mol) solutions and known quantity of PAC was added to it. The suspension was stirred at 70 °C with dropwise addition of NaOH solution ($5\,mol\,L^{-1}$). The final product was washed with distilled water to attain a pH 6.5. It was filtered, and dried in an oven at 100 °C for 6 h. The physical parameters of MAC13 were measured (Table 3). Pure iron oxide was also produced from the same amounts of $FeCl_3$ (28 m mol) and $FeSO_4$ (14 m mol) at 70 °C following the same route as mentioned above for understanding the differences in the structure of PAC and MAC13. The PAC, MAC13, and iron oxide were characterized by XRD (Rigaku D/Max-2,200/PC). Iron oxide and MAC13 composite were characterized by bulk sigma magnetization (Vibrating Sample Magnetometer [VSM]). The BET surface area of PAC and MAC13 were determined by a surface area analyzer QS-7 by standard N_2 adsorption at 77 K.

The equilibrium adsorption experiments were carried out by immersing 0.01 g PAC and MAC13 with 100 mL of Triton X-100 (pH = 7.5), SDBS (pH = 8.3), and N-dodecylpyridinium chloride (pH = 4.5) solutions

Table 1
UF membrane parameters

Parameter	Specification
Material	Polyethersulfone
Type	Capillary multibore × 7
Diameter bores ID	0.9 mm
Diameter fibre OD	4.2 mm
MWCO	100 kD
Surface area	$50\,m^2$
Maximum temperature	40 °C
Maximum pressure	7.5 bar
Membrane back wash pressure	0.5–1 bar
Maximum	2.5 bar
Operation pH range	3–10
Back wash pH range	1–13
Disinfection chemicals	
Hypochlride (NaOCl)	$50–200\,mg\,L^{-1}$
Hydrogen peroxide (H_2O_2)	$100–200\,mg\,L^{-1}$

containing various initial concentrations (10–100 mg L^{-1}) of adsorbate and stirring at 250 rpm for 12 h in a thermostat cum shaking assembly at 25 °C. The adsorbate solutions were separated from the adsorbents by centrifugation and their concentrations were determined by UV–Visible spectrophotometer (Thermo Electron corporation Heγios γ UV–Visible spectrophotometer) at 275, 223.5, and 213.5 nm for Triton X-100, SDBS, and N-dodecylpyridinium chloride, respectively. The adsorption capacities of adsorbates were calculated by the following equations:

$$q = (C_0 - C) \quad \mathrm{V/m}$$

where q is equilibrium adsorption capacity (mg g^{-1}), C_0 and C are the initial and equilibrium concentration of adsorbate solution (mg L^{-1}), V is volume of solution (L), and m is mass of adsorbent used. The extents of adsorption by plastic bottles used in the experiment were determined. No appreciable adsorption of the adsorbates was observed at room temperature. However, at 50 °C and 13 days contact time, the adsorption was appreciable.

The adsorption kinetic experiments were performed in a specially designed container of 12 L capacity. Mixing was provided by a blade. A motor was used to drive the impeller. The top surface of the vessel was open to atmosphere. Experiments were performed at the agitation rate of 250 rpm and 25 °C. Samples were withdrawn at different time intervals using syringe and were analyzed by UV–Visible spectrophotometer.

The membranes were initially rinsed with distilled water for 1 h. Solutions of known concentration of the Triton X-100, SDBS, and N-dodecylpyridinium chloride were prepared in distilled water. All samples were equilibrated to room temperature and 1.0 bar pressure was maintained throughout the experimental cycle. The percent retention of the solute R was determined by using following formula:

$$R = 100\left(1 - \frac{C_p}{C_b}\right)$$

Table 2
Physical properties of PAC

Parameter	Specification
BET surface area	1,150 $m^2 g^{-1}$
Micropore volume	0.335 $cm^3 g^{-1}$
Mesopore volume	0.085 ($cm^3 g^{-1}$)
Apparent density	0.51 g mL^{-1}
Particle size	
d10	4 μm
d50	24 μm
d90	90 μm
Ash	12% Max
Chloride (acid extracts)	0.1%
pH	Alkaline

Table 3
Physical properties of MAC13 and iron oxide

Material	Surface area ($m^2 g^{-1}$)	Micropore volume ($cm^3 g^{-1}$)	Mesopore volume ($cm^3 g^{-1}$)
Magnetic activated carbon (1:3)	1,020	0.295	0.080
Iron oxide	64	0.07	–

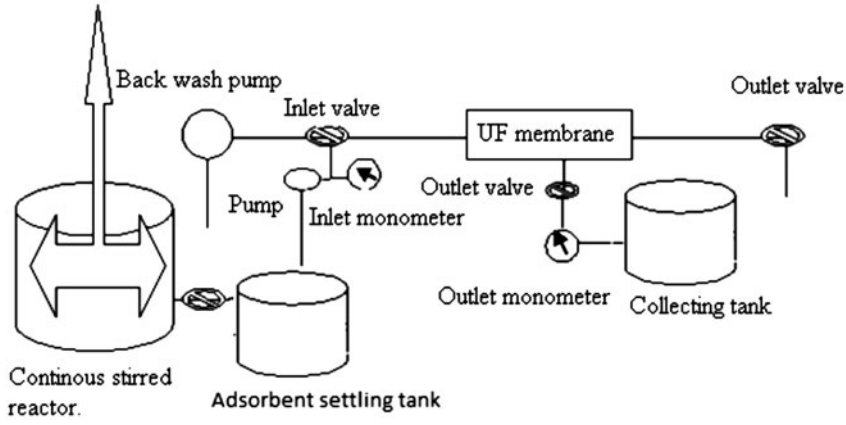

Fig. 1. Diagram of UF system.

where C_p is the concentration of solute in permeate and C_b is the solute concentration in bulk.

Membrane flux averaged over time of filtration was calculated as follow:

$$j = \frac{1}{A}\frac{dV}{dt}$$

where A is the membrane area and V is the permeate volume at time t.

Then, the membrane was used in combination with continuous stirred reactor, where PAC and MAC13 were added to the adsorbate solutions in a single dose and were stirred for 1 h before feeding to the membrane system. The UF membrane system was operated in dead end mode. In case of MAC13, a specially designed container equipped with magnetic arrangement was put in the assembly (Fig. 1).

3. Results and discussion

3.1. Characterization of adsorbents

3.1.1. Surface area of adsorbents

The iron oxide/PAC composite (1:2) reported in our previous work has lower surface area as compared to PAC [33]. The presence of iron oxide in the composite structure affect the BET surface area and micropore volume due to presence of 33% iron contents, a drop in the surface area was observed. In order to increase the surface area of iron oxide/PAC composite, in this study a 1:3 iron oxide/PAC composite was prepared. The surface areas of PAC and MAC13 were determined by standard N_2 adsorption at 77 K (Tables 2 and 3). It can be seen from Tables 2 and 3 that the magnetization process affects the surface area and values of micro-pore structure of the PAC. This is due to impregnation of iron oxide on PAC particles and the resulting composite MAC13 has low surface area as compared to PAC.

3.1.2. XRD analysis

PAC, MAC13, and iron oxide were characterized by XRD. Four iron oxides are formed under reaction condition, magnetite (Fe_3O_4), maghemite (γ-Fe_2O_3), hematite (α-$Fe_2O_{3)}$, and goethite (α-FeO(OH)). To get high surface area composite, the iron oxide contents must be decreased. However, by decreasing the iron oxide to PAC ratio caused a loss of magnetite and maghemite took place by air oxidation. To prevent air oxidation of MAC13 composite, the reaction was carried out under inert atmosphere of nitrogen. The XRD

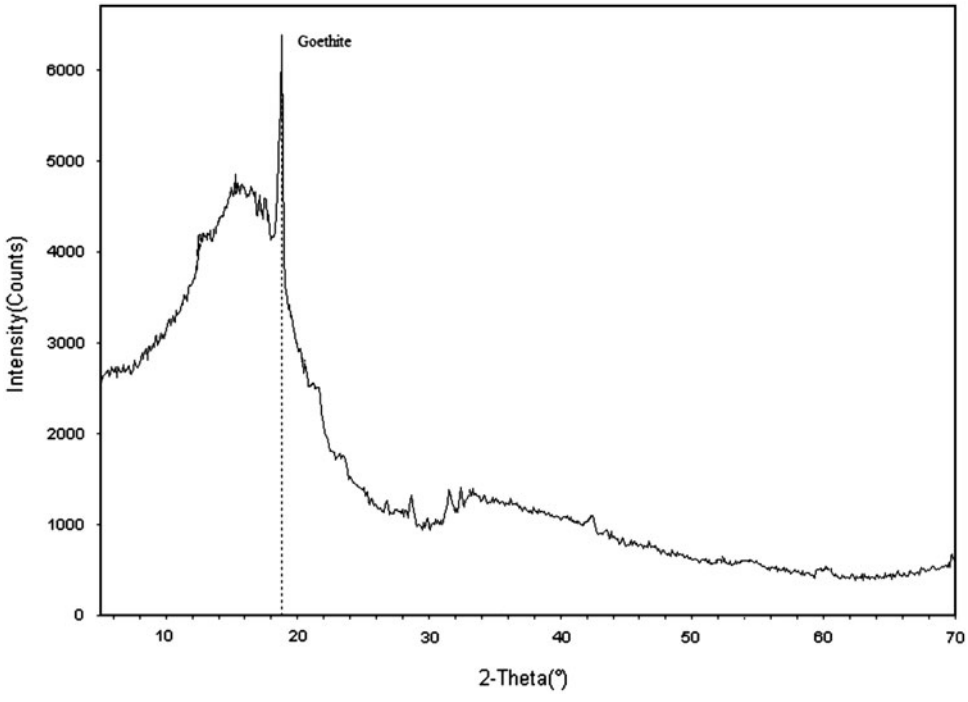

Fig. 2. X-ray patterns of PAC.

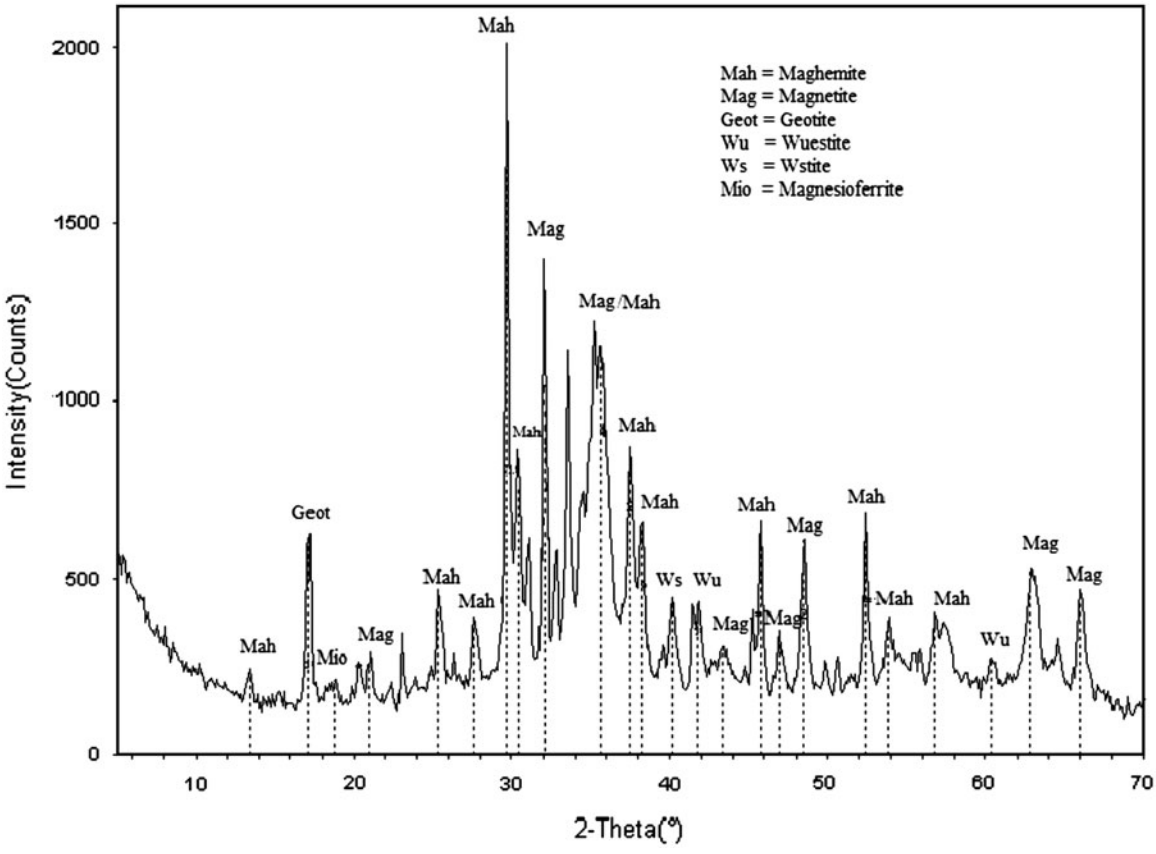

Fig. 3. X-ray patterns of iron oxide sample.

patterns of PAC, MAC13, and iron oxide are given in Figs. 2–4. Magnetite and maghemite are the iron oxides attracted by magnet. The XRD pattern of MAC13 shows the presence of maghemite.

3.1.3. Vibrating sample magnetometer analysis

According to Olivira et al. [34] an increase in the iron oxide contents in the composite increases bulk sigma magnetization. However, this increase is not proportional to iron oxide contents. With the increase in activated carbon contents, there is an increase in non-magnetic oxide concentration. Our goal is to prepare such a magnetic adsorbent having surface area comparable to PAC and high magnetic oxide contents. By carrying out the reaction under inert atmosphere of nitrogen, the magnetic contents of the composite can be improved. When the reaction was carried out under atmospheric conditions, there were no measureable magnetic oxide contents in the composite. Fig. 5 shows bulk magnetization of iron oxide sample while Fig. 6 indicates bulk magnetization of MAC13 composite. From the given figures, the magnetic values of iron oxide and MAC13 composite are 77 and 68 emu g^{-1}, respectively. The lower magnetization of composite is probably due to the presence of PAC in the MAC13 composite. The 1:4 and 1:5 composites were also prepared, but there magnetization values were lower than 40 emu g^{-1} and were not attracted by the magnet.

3.1.4. Adsorption isotherms

The equilibrium data for the adsorption of Triton X-100, SDBS, and N-dodecylpyridinium chloride on PAC and MAC13 were analyzed by Langmuir and Freundlich models [35,36]. The linear form of Langmuir adsorption isotherm is given as follow:

$$\frac{C}{q} = \frac{C}{Q_0} - \frac{1}{Q_0 b}$$

where q is the amount adsorbed (mg g^{-1}) and C is the equilibrium concentration of the adsorbate (mg L^{-1}). Q_0 and b are Langmuir constants related to maximum

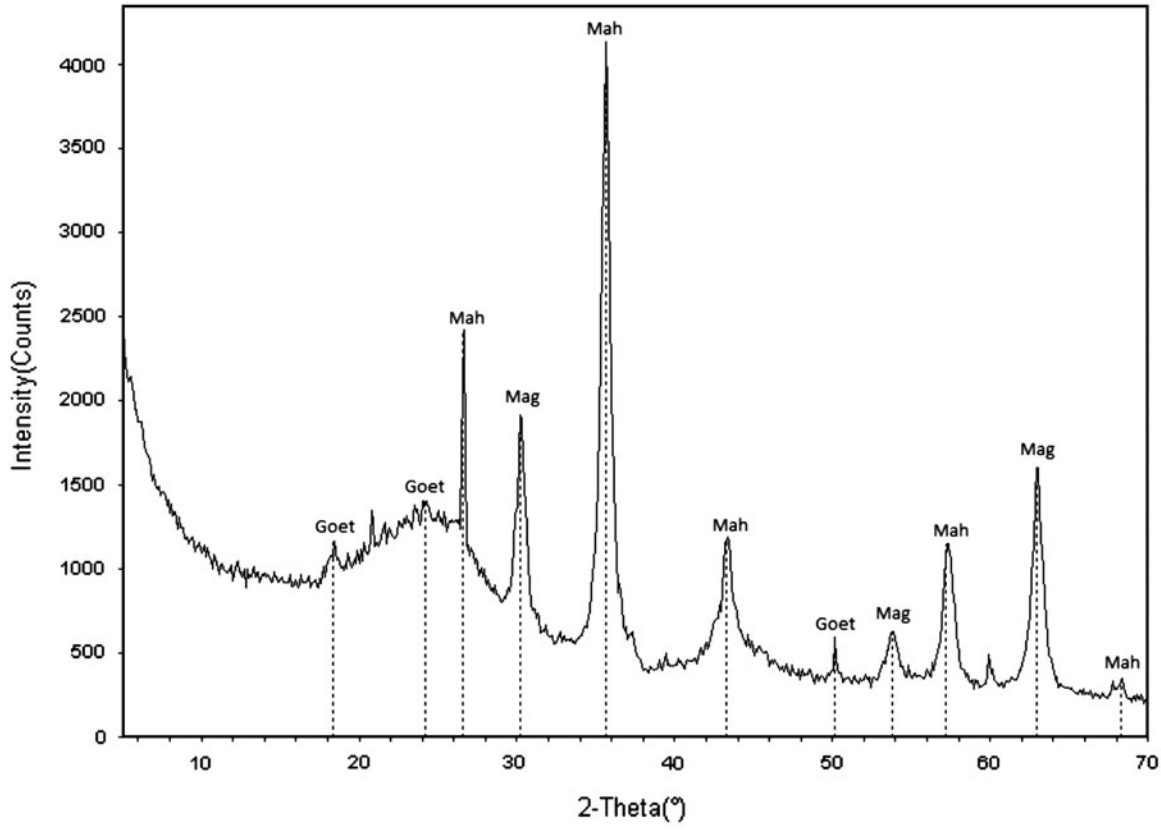

Fig. 4. X-ray patterns of MAC13.

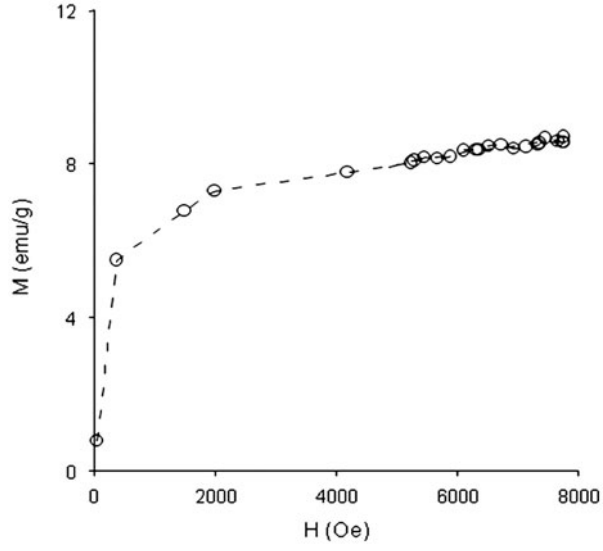

Fig. 5. Bulk sigma magnetization for iron oxide.

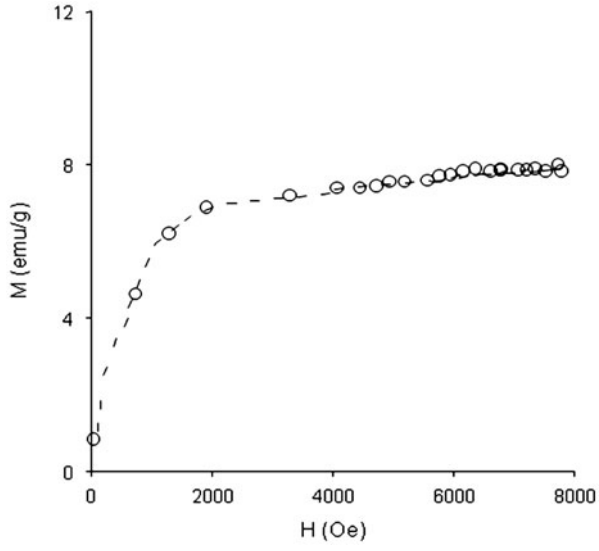

Fig. 6. Bulk sigma magnetization for MAC13 composite.

adsorption capacity and energy of adsorption, respectively. The adsorption constants were calculated from slope and intercept of the C/q vs. C plot. The values of adsorption constants are given in Table 4. The logarithmic form of Freundlich adsorption isotherm is given as

Table 4
Isotherm parameters for adsorption of Triton X-100, SDBS, and N-dodecylpyridinium chloride on PAC and MAC13

Isotherm	PAC			MAC13		
	Triton X-100	SDBS	N-dodecylpyridinium chloride	Triton X-100	SDBS	N-dodecylpyridinium chloride
Langmuir						
Q_0 (mg g^{-1})	204.9	215.9	238.89	137.15	196.3	121.16
b (L mg^{-1})	0.018	0.16	0.89	0.036	0.39	0.105
R^2	0.976	0.99	0.999	0.98	0.998	0.99
Freundlich						
K	8.9	67.6	71.8	11.5	88.78	22.9
$1/n$	0.596	0.265	0.128	0.519	0.2	0.388
R^2	0.97	0.946	0.845	0.947	0.968	0.84

$$\ln q = \ln K + \frac{1}{n} \ln C$$

where C is the equilibrium concentration (mg L^{-1}) and q is the amount adsorbed (mg g^{-1}). K and n are Freundlich constants related to adsorption capacity and adsorption intensity, respectively. The values of K and n can be calculated from intercept and slope of ln q vs. ln C plot.

The adsorption capacities of Triton X-100, SDBS, and N-dodecylpyridinium chloride on MAC13 increase in the given order, Triton X-100 < SDBS < N-dodecylpyridinium chloride. The same trend was observed for PAC. The adsorption capacities of these surfactants for PAC were higher than MAC13. The lower adsorption capacity of MAC13 is due to impregnation of iron oxide in the micropores of PAC. Iron oxide has low surface area, which decreases the total surface area of the MAC13 as compared to PAC. The values of n are within the expected range from 1 to 10 which signifies favorable adsorption.

3.1.5. Adsorption kinetics

The adsorption kinetics is important for determining the adsorption mechanism. A number of models are used to analyze the adsorption kinetics data. Amongst them, the pseudo-first-order and second-order kinetics models are more frequently used [37,38]. The pseudo-first-order model can be expressed by following relation:

$$\ln(q_e - q) = \ln q_e - K_a t$$

where q_e and q (mg g^{-1}) are the amount of sorbed adsorbate at equilibrium and time t, respectively, and K_a (min^{-1}) is the rate constant. This equation shows a linear relationship between $\ln(q_e - q)$ and t.

The pseudo-second-order equation is given as

$$\frac{t}{q_t} = \frac{1}{K_2 q^2} + \left(\frac{1}{q}\right) t$$

where K_2 (g mg^{-1} min^{-1}) is the rate constant of adsorption, q (mg g^{-1}) is the amount of adsorbate adsorbed at equilibrium and q_t at time t. The pseudo-first-order and second-order rate constants and co-relation constants for the adsorption of Triton X-100, SDBS, and N-dodecylpyridinium chloride on PAC and MAC13 are given in Table 5. The result in table shows that the R^2 values are high for pseudo-second-order kinetic model as compared to the pseudo-first-order kinetic model. This indicates that the adsorption of Triton X-100, SDBS, and N-dodecylpyridinium chloride onto PAC and MAC13 obeys the pseudo-second-order kinetics model. From table, it is also evident that the values of K_a and K_2 are higher for MAC13 as compared to PAC. It clearly indicates that the impregnation of iron oxide increases the rate of adsorption of Triton X-100, SDBS, and N-dodecylpyridinium chloride on PAC and MAC13.

3.1.6. UF/adsorption

Concentration polarization and fouling by organic substances affect the efficiencies of the ultra membrane processes. The decline in flux due to concentration polarization occurs in a very short time and after this rapid drop, the flux remains constant with the passage of time. A gradual reduction in flux has been observed in long-term applications due to fouling. There are three major causes of fouling; cake formation over the membrane surface, pore blocking,

Table 5
Kinetic parameters for the adsorption of surfactants onto PAC and MAC13 at 25 °C

Adsorbent	Surfactant	Pseudo first order kinetic model		Pseudo second order kinetic model	
		K_a (min^{-1})	R^2	K_2 ($min\,g\,mg^{-1}$)	R^2
PAC	Triton X-100	0.025	0.987	8.3×10^{-4}	0.999
	SDBS	0.022	0.884	4.3×10^{-3}	0.998
	N-dodecylpyridinium chloride	0.025	0.758	8.0×10^{-3}	0.999
MAC13	Triton X-100	0.055	0.881	2.0×10^{-3}	0.98
	SDBS	0.080	0.924	4.37×10^{-3}	0.996
	N-dodecylpyridinium chloride	0.055	0.944	7.8×10^{-3}	0.997

and adsorption. The pore blocking may be complete blocking, intermediate blocking, or standard blocking. The first two blockages are due to molecules larger than the size of the membrane pores or having a comparative size to that of the membrane pores while the later blocking occurs due to the adsorption of smaller molecules within the pores [32,39].

In PAC/UF hybrid processes, PAC enters into membrane system forming cake over membrane surface and causes a decline in permeate flux. Frequent back washes are needed to restore membrane efficiency which results in loss of water and electricity. PAC also causes blackening of pipes and other accessories of the membrane system which needs replacement after some time. In our previous work, a magnetic adsorbent MAC was prepared and used for foul control in membrane processes. The prepared adsorbent was an iron oxide and PAC composite in 1:2 ratio. The impregnation of iron oxide in the pores of PAC results in low surface area of the composite. Although improved flux and percent retention of organic substances were observed when used in combination with UF membrane. However, the decline in flux due to cake formation by PAC was compensated by its high surface area. As a result, improved fluxes were observed for PAC in comparison to MAC [33].

To prepare MAC composite having high surface area, the PAC to iron oxide ratio was raised to 1:3, 1:4, and 1:5. The magnetization value for 1:4 and 1:5 composite were lower than 40 emu g^{-1} and were not attracted by magnet. Thus, 1:3 was found to be the optimal ratio. The 1:3 composite was used in combination with UF membrane. The various UF/adsorption parameters are discussed in detail as below.

3.1.7. Retention of surfactants

The retention of the solute R by UF membrane depends on its size and configuration relative to the pore size. Chemical interactions of the solution and membrane like adsorption, concentration polarization, and fouling are also important [33]. The percent retention of Triton X-100, SDBS, and N-dodecylpyridinium chloride by membrane alone is given in Fig. 7 while with PAC/UF and MAC13/UF hybrid processes are given in Figs. 8 and 9. The percent retention of Triton X-100, SDBS, and N-dodecylpyridinium chloride by membrane was lower as compared to PAC/UF and MAC13/UF hybrid processes. The percent retention was high for cationic surfactant N-dodecylpyridinium chloride as compared to anionic surfactant SDBS and Triton X-100.

3.1.8. Effects of adsorbents on permeate flux

The decline in the permeate flux in the initial stages for water was due to the intrinsic membrane

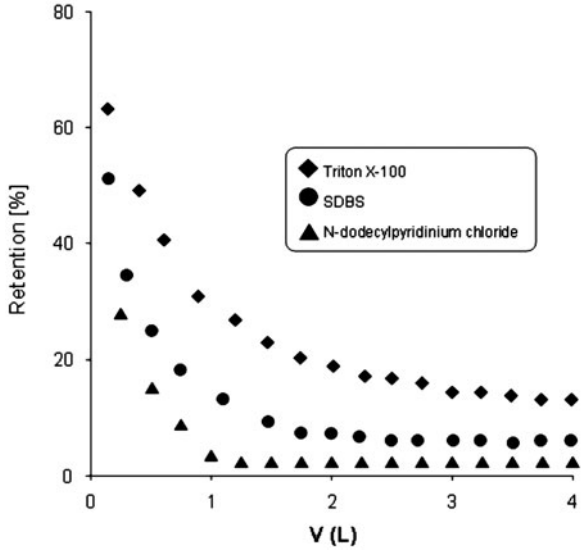

Fig. 7. Retention of Triton X-100, SDBS, and N-dodecylpyridinium chloride by UF membrane.

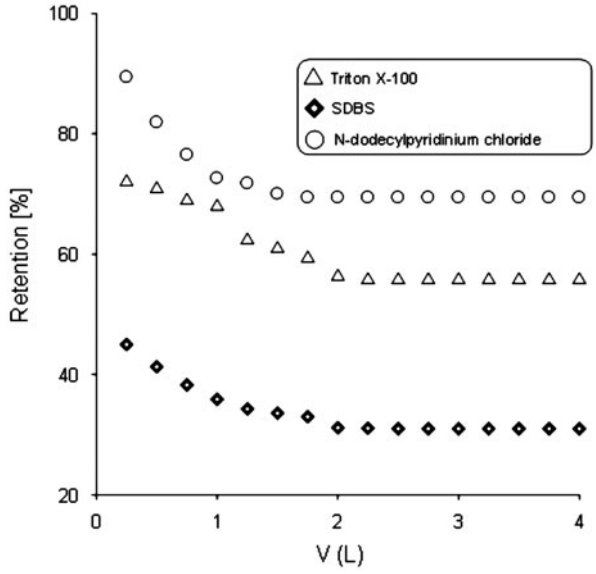

Fig. 8. Retention of Triton X-100, SDBS, and N-dodecylpyridinium chloride in PAC/UF hybrid system.

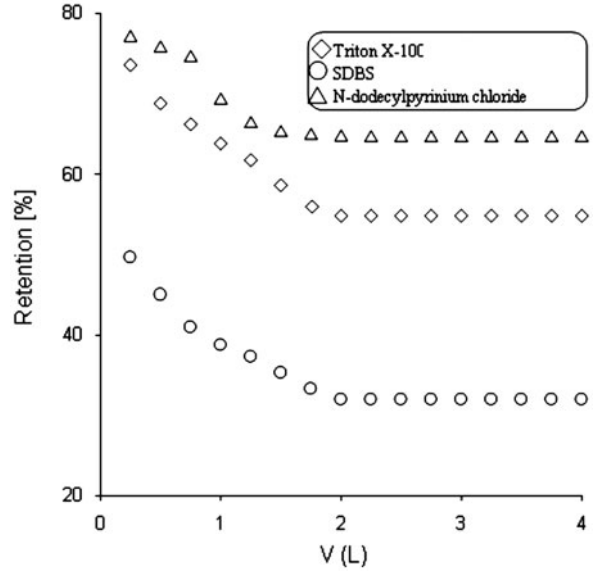

Fig. 9. Retention of Triton X-100, SDBS, and N-dodecylpyridinium chloride in MAC13/UF hybrid system.

resistance and interaction of the ions present in distilled water with membrane. The flow rate then reached a steady state and was no longer affected within the experimental cycle. The molecular weights of these surfactants under study were smaller than the molecular weight cut off (MWCO) of the membrane. These substances were expected to pass freely from the membrane and allow the permeate concentration equal to that of the bulk concentration. However,

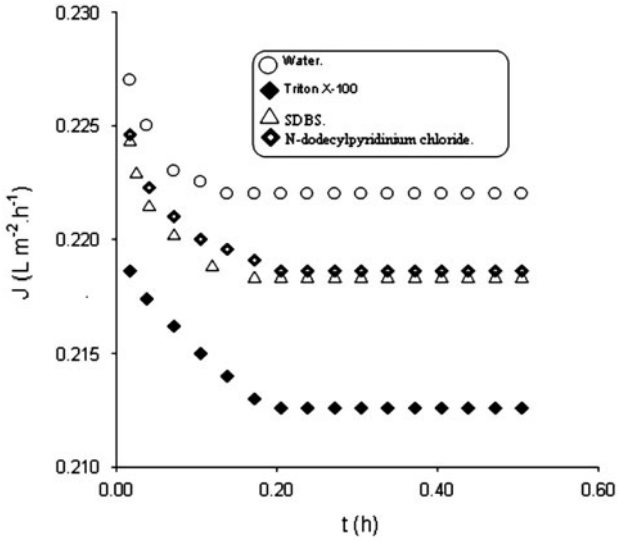

Fig. 10. Influence of Triton X-100, SDBS, and N-dodecylpyridinium chloride on permeate flux.

despite of low retention, flux reduction was observed for these substances. This was due to adsorption of these surfactants in the pores of the membrane that causes gradual reduction in permeating flux. The reduction in permeate flux was high for cationic surfactant N-dodecylpyridinium chloride as compared to anionic surfactant SDBS. For non-ionic surfactant Triton X-100, the reduction in permeate flux was minimum. This was due to high adsorption of N-dodecylpyridinium chloride and SDBS on membrane surface as compared to Triton X-100. The adsorption of these substances over membranes partially blocks the pores of membrane resulting in low fluxes.

The influence of PAC and MAC13 on permeate fluxes of Triton X-100, SDBS, and N-dodecylpyridinium chloride are shown in Figs. 10–12. Although MAC13 has low surface area as compared to PAC, improved permeate fluxes were observed for MAC13, as PAC causes cake formation over the membrane surface which reduces permeate flux. Thus, the lower surface area of MAC13 was compensated by no cake formation on membrane surface and improved fluxes were observed.

3.1.9. Effect of adsorbents on back wash times

After each 30 min cycle, cleaning with deionized distilled water was practiced. For PAC, the back wash time was high as compared to MAC13. This is due to the complete removal of MAC13 from slurry in the settling tank. For PAC, the complete removal was not possible and as a result, cake formation took place

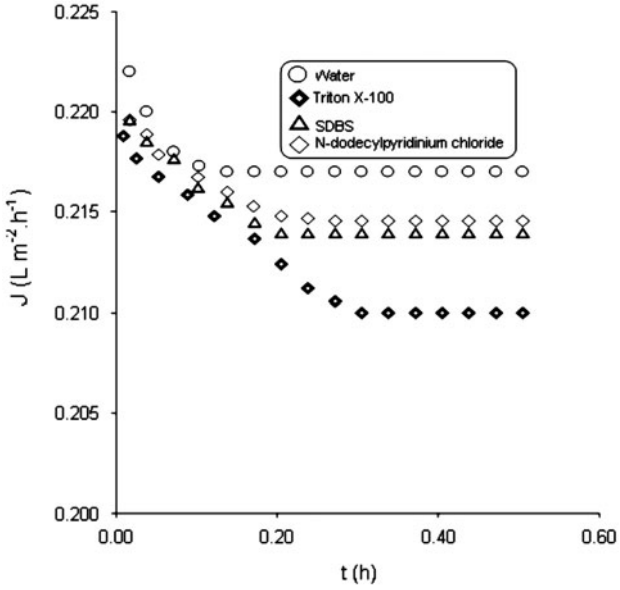

Fig. 11. Influence of Triton X-100, SDBS, and N-dodecylpyridinium chloride on permeate flux in presence of MAC13.

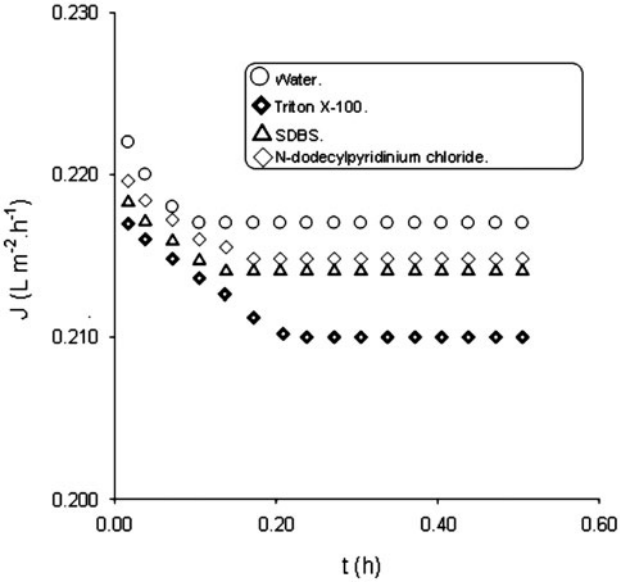

Fig. 12. Influence of Triton X-100, SDBS, and N-dodecylpyridinium chloride on permeate flux in presence of PAC.

over the membrane surface which lengthens the back wash times. For PAC, blackening of the pipes and flow meter of the membrane system were also observed. From an economical point of view, the use of PAC in the membrane systems is expensive as compared to MAC13 as it reduces backwash times and does not cause blackening of the pipes.

4. Conclusions

The MAC13 composite prepared in this study was compared with PAC for its adsorptive capacities. The PAC has high surface area as compared to MAC13 due to impregnation of iron oxide in the pores of PAC. The equilibrium data fit well to Langmuir adsorption isotherm rather than Freundlich adsorption isotherm. The kinetics data fit well to pseudo-second-order kinetic model. High percent retention of Triton X-100, SDBS, and N-dodecylpyridinium chloride was observed with PAC in PAC/UF process. It was due to efficient absorptive capacities of PAC for adsorbates under study. However, improved permeate fluxes were observed for MAC13. It was due to the removal of MAC13 from slurry by magnet and thus encounters no cake formation on membrane surface, as was observed for PAC.

Acknowledgment

The study was supported by research fund of Istanbul University Project no: 3822.

References

[1] Adak, M. Bandyopadhyay, A. Pal, Removal of anionic surfactant from wastewater by alumina: A case study, Colloids Surf. A 254 (2005) 165–171.
[2] E. Onder, A.S. Koparal, U.B. Ogutveren, An alternative method for the removal of surfactants from water: Electrochemical coagulation, Sep. Purif. Technol. 52 (2007) 527–532.
[3] C.S. Rao, Environmental Pollution Control Engineering, Wiley Eastern Ltd., New Delhi, 1991, pp. 165–232.
[4] G. Lissens, J. Pieters, M. Verhaege, L. Pinoy, W. Verstraete, Electrochemical degradation of surfactants by intermediates of water discharge at carbon-based electrodes, Electrochim. Acta 48 (2003) 1655–1663.
[5] S. Mozia, M. Tomaszewska, A.W. Morawski, Decomposition of nonionic surfactant in a labyrinth flow photoreactor with immobilized TiO_2 bed, Appl. Catal. B 59 (2005) 155–160.
[6] B. Shiau, J.H. Harwell, J.F. Scamehorn, Precipitation of mixtures of anionic and cationic surfactants: III. Effect of added nonionic surfactant, J. Colloid Interface Sci. 167 (1994) 332–345.
[7] F.I. Talens-Alesson, S.T. Hall, N.P. Hankins, B. Azzopardi, Flocculation of SDS micelles with Fe^{3+}, J. Colloids Surf. 204 (2002) 85–91.
[8] N.N. Rao, S. Dube, Photocatalytic degradation of mixed surfactants and some commercial soap/detergent products using suspended TiO_2, J. Mol. Catal. 104 (1996) 197–199.
[9] M. Ohtaki, H. Sato, H. Fujii, K. Eguchi, Intramolecularly selective decomposition of surfactant molecules on photocatalytic oxidative degradation over TiO_2 photocatalyst, J. Mol. Catal. 155 (2000) 121–129.
[10] T. Zhang, T. Oyama, S. Horikoshi, J. Zhao, N. Serpone, H. Hidaka, Photocatalytic decomposition of the sodium dodecylbenzene sulfonate surfactant in aqueous titania suspensions exposed to highly concentrated solar radiation and effects of additives, Appl. Environ. 42 (2003) 13–24.
[11] M. Ogita, Y. Nagai, M.A. Mehta, T. Fujinami, Application of the adsorption effect of optical fibres for the determination of critical micelle concentration, Sens. Actuat. 64 (2000) 147–151.
[12] A. Adak, M. Bandyopadhyay, A. Pal, Removal of anionic surfactant from wastewater by alumina: A case study, Colloids Surf. 254 (2005) 165–171.

[13] Y. Lin, T.W. Smith, P. Alexandridis, Adsorption of a polymeric siloxane surfactant on carbon black particles dispersed in mixtures of water with polar organic solvents, J. Colloid Interface Sci. 255 (2002) 1–9.
[14] J.S. Matthew, N.J. Malcolm, The biodegradation of surfactants in the environment, Biochim. Biophys. Acta Biomembr. 1508 (2000) 235–251.
[15] H.J. Chen, D.H. Tseng, S.L. Huang, Biodegradation of octylphenol polyethoxylate surfactant Triton X-100 by selected microorganisms, Bioresour. Technol. 96 (2005) 1483–1491.
[16] A. Dhouib, N. Hamad, I. Hassaïri, S. Sayadi, Degradation of anionic surfactants by *Citrobacter braakii*, Process Biochem. 38 (2003) 1245–1250.
[17] J. Sirieix-Plénet, M. Turmine, P. Letellier, Membrane electrodes sensitive to doubly charged surfactants. Application to a cationic gemini surfactant, Talanta 60 (2003) 1071–1078.
[18] E. Fernández, J.M. Benito, C. Pazos, J. Coca, Ceramic membrane ultrafiltration of anionic and nonionic surfactant solutions, J. Membr. Sci. 246 (2005) 1–6.
[19] I. Kowalska, M. Kabsch-Korbutowicz, K. Majewska-Nowak, T. Winnicki, Separation of anionic surfactants on ultrafiltration membranes, Desalination 162 (2004) 33–40.
[20] M.R. Wiesner, M.M. Clark, J. Mallevialle, Membrane filtration of coagulated suspensions, J. Environ. Eng. 115 (1989) 20–40.
[21] V. Lahoussine-Turcaud, M.R. Wiesner, J. Bottero, Mallevialle Coagulation pretreatment for ultrafiltration of a surface water, Am. Water Works Assoc. J. 82 (1990) 76–81.
[22] T. Carroll, S. King, S.R. Gray, B.A. Bolto, N.A. Booker, The fouling of microfiltration by NOM after coagulation treatment, Water Res. 34 (2000) 2861–2868.
[23] A. Braghetta, J.G. Jacangelo, S. Chellem, M.L. Hotaling, B.A. Utne, DAF pretreatment: its effect on MF performance, Am. Water Works Assoc. J. 89 (1997) 90–101.
[24] S.S. Adham, V.L. Snoeyink, M.M. Clark, J. Bersillon, Predicting and verifying organics removal by PAC in an ultrafiltration system, Am. Water Works Assoc. J. 83 (1991) 81–91.
[25] J.G. Jacangelo, J. Laine, E.W. Cummings, S.S. Adham, UF with pretreatment for removing DPB precursors, J. Am. Water Works Assoc. 87 (1995) 100–112.
[26] K. Konieczny, G. Klomfas, Using activated carbon to improve natural water treatment by porous membranes, Desalination 147 (2002) 109–116.
[27] J.M. Laıne, D. Vial, P. Moulart, Status after 10 years of operation – overview of UF technology today, Desalination 131 (2000) 17–25.
[28] R. Pianta, M. Boller, M.L. Janex, A. Chappaz, B. Birou, R. Ponce, Micro- and ultra-filtration of karstic spring water, Desalination 117 (1998) 61–71.
[29] L. Qilin, V.L. Snoeyink, B.J. Marinas, C. Campos, Pore blockage effect of NOM on atrazine adsorption kinetics of PAC: The roles of PAC pore size distribution and NOM molecular weight, Water Res. 37 (2003) 4863–4872.
[30] S.J. Lee, K.H. Choo, C.H. Lee, Conjunctive use of ultrafiltration with powdered activated carbon adsorption for removal of synthetic and natural organic matter, J. Ind. Eng. Chem. 6 (2000) 357–364.
[31] C.F. Lin, S.H. Liu, O.J. Hao, Effect of functional groups of humic substances on UF performance, Water Res. 35 (2001) 2395–2402.
[32] C.F. Lin, Y.J. Huang, O.J. Hao, Ultrafiltration processes for removing humic substances: Effect of molecular weight fractions and PAC treatment, Water Res. 33 (1999) 1252–1264.
[33] M. Zahoor, M. Mahramanlioglu, Removal of phenolic substances from water by adsorption and adsorption–ultrafiltration, Sep. Sci. Technol. 46 (2011) 1482–1494.
[34] L.C.A. Oliveira, R.V.R.A. Rios, J.D. Fabris, V. Garg, K. Sapag, R.M. Lago, Activated carbon/iron oxide magnetic composites for the adsorption of contaminants in water, Carbon 40 (2002) 2177–2183.
[35] I. Langmuir, The adsorption of gases on plane surfaces of glass, mica and platinum, J. Am. Chem. Soc. 40 (1918) 1361–1403.
[36] H. Freundlich, Über die adsorption in lösungen [Adsorption in solution], Z. Phys. Chem. 57 (1906) 384–470.
[37] S. Lagergren, Zur theorie der sogenannten adsorption geloester stoffe [Kinetics equation for solute adsorption on various adsorbents], Kungliga Svenska Vetenskapsakad, Handlingar 24 (1898) 1–39.
[38] Y.S. Ho, G. Mckay, Sorption of dye fromaqueous solution by peat, Chem. Eng. J. 70 (1998) 115–124.
[39] A.S. Jonsson, J. Lindau, J. Brink, B. Jonsson, Influence of the concentration of a low-molecular organic solute on the flux reduction of a polyethersulfone ultrafiltration membrane, J. Membr. Sci. 135 (1997) 117–128.